Hindawi
Journal of Electrical and Computer Engineering
Volume 2023, Article ID 5566965, 11 pages
https://doi.org/10.1155/2023/5566965

Research Article

Lithium-Ion Battery State-of-Health Estimation Method Using Isobaric Energy Analysis and PSO-LSTM

Shaishai Zhao,[1] Laijin Luo,[1] Shanhe Jiang,[1] and Chaolong Zhang[2]

[1]*School of Electronic Engineering and Intelligent Manufacturing, Anqing Normal University, Anqing 246011, China*
[2]*College of Intelligent Science and Control Engineering, Jinling Institute of Technology, Nanjing 211169, China*

Correspondence should be addressed to Shanhe Jiang; jshxlxlw@163.com and Chaolong Zhang; zhangchaolong@126.com

Received 25 February 2023; Revised 4 August 2023; Accepted 28 August 2023; Published 11 September 2023

Academic Editor: Luigi Piegari

The precise estimation of the state of health (SOH) for lithium-ion batteries (LIBs) is one of the core problems for battery management systems. To address the problem that it is difficult to accurately evaluate SOH because of the LIB capacity regeneration phenomenon, this paper proposes an approach for LIB SOH estimation using isobaric energy analysis and improved long short-term memory neural network (LSTM NN). Specifically, at first, the isobaric energy curve is plotted by analyzing the battery energy variation during the constant current charging stage. Then, the mean peak value of the isobaric energy curve is extracted as a health factor to characterize the battery SOH aging. Eventually, the LIB SOH estimation model is developed using the improved LSTM NN. In this regard, the improved LSTM NN refers to the selection of the number of hidden layers and the learning rate of the LSTM NN using the particle swarm algorithm (PSO). To verify the precision of the proposed method, validation experiments are performed based on four battery aging data with different charging multipliers. The experimental results indicate that the proposed method can effectively estimate the LIB SOH. Meanwhile, the proposed method is compared with other conventional machine learning algorithms, which demonstrates that the proposed method has better estimation performance.

1. Introduction

Lithium-ion batteries (LIBs) have been implemented in a variety of application scenarios, from smart grids to aerospace and electric vehicles. This is attributed to its merits such as high energy density, long cycle life, and low self-discharge rate [1–3]. However, the LIB state of health (SOH) continues to decrease during the continued service of LIBs. As a result, the LIB SOH can be used as an important indicator to diagnose the degree of battery aging. Nevertheless, due to the complexity and diversity of the aging parameters of LIBs [4], it is challenging to accurately predict the LIB SOH. In recent years, many scholars have devoted themselves to SOH estimation techniques for LIBs. These techniques can be broadly classified into model-based and data-driven techniques [5].

The model-based methodology implies constructing a simulation model of LIB as a way to simulate the chemical reactions occurring inside the battery during its operation. Three commonly accepted equivalent models for LIBs are the electrochemical mechanism model, the equivalent circuit model, and the empirical degradation model [6–8]. For example, Xiong et al. [9] proposed a simplified pseudo-two-dimensional model using a finite analysis method. Mevawalla et al. [10] developed a simplified electrochemical thermal model involving a large number of partial differential equation calculations. Yang et al. [11] proposed an equivalent circuit model and improved the accuracy of the model by using parallel connections. Zheng et al. [12] proposed a feedforward empirical model and combined it with a feedback neural network to predict the battery capacity. However, owing to the complex computational process and parameters of the model-based approach, it is often not easy to implement in real-time monitoring of the battery management system.

Instead of analyzing the internal electrochemical reactions of LIBs, the data-driven approach investigates the historical data from experimental measurements [13] and then builds a LIB SOH estimation model from the extracted current and voltage characteristics. Commonly employed data-driven methods include support vector machine (SVM) [14], extreme learning machine (ELM) [15], relevance vector regression (RVR) [16], and long short-term memory neural network (LSTM NN) [17]. Among them, the input weights of the ELM algorithm are random and cannot be fine-tuned for changes in data features, which is less controllable and the output results of the model are unstable [18]. The SVM method is difficult to divide large-scale data samples, and the computational cost will be greatly increased, which requires the selection of regularization parameters, kernel function, and kernel function parameters [15]. Although the accuracy of the RVR approach is similar to the SVM in regression and classification tasks, the training time is shorter. In addition, the RVR approach can be more generalized and more suitable for online prediction scenarios [19]. LSTM NN can well learn historical and future information so as to overcome the difficulty of accurate model of LIB SOH caused by the capacity regeneration problem in practical applications of LIB. In addition, the gradient disappearance of the traditional recurrent neural network is addressed in long-term sequence prediction, which effectively improves the generalization and robustness of the network model [20].

Although the data-driven approach can deal with the nonlinearity problem well, the model estimation accuracy depends on the analysis and extraction of features. By analyzing the relationship between battery aging characteristics and charging time, Lin et al. [21] estimated SOH accurately. The voltage difference within a fixed time difference was extracted by Liu and Chen [22] during constant current and constant voltage charging stages as a health characteristic for SOH estimation. Goh et al. [23] split the discharge process into various phases based on the curvature of the discharge curve and extracted many HIs with a high correlation to battery SOH in the discharge platform stage of the discharge curve. Shu et al. [24] proposed to simultaneously achieve the estimation of state of health and optimize the healthy features therein, which are excavated based on the charging voltage curves within a fixed range.

The above methods extract features from charging curves, and the extracted features cannot indicate the internal violent reaction process of the battery [25, 26]. In recent years, incremental capacity analysis (ICA) has been widely used to analyze battery aging characteristics and extract features. Guo et al. [27] used the maximum value of the IC curve, the corresponding voltage, and the energy and the capacity of a constant current charging interval determined by the maximum value of the IC curve to estimate the battery SOH. Based on calendar aging results collected during 11 months of testing, Stroe and Schaltz [28] were able to relate the capacity fade of the studied batteries to the evolution of four metric points, which were obtained using the ICA. Zhang et al. [29] proposed the ICA method and improved the broad learning system network-based SOH estimation technology for lithium-ion batteries. The experimental results demonstrate that the proposed method can effectively evaluate the SOH with strong robustness. Li et al. [30] used Gaussian filtering to extract the feature of the IC curve after smoothing the static charging curve and then derived the mapping relationship, but there is a large measurement error noise interference resulting in poor SOH estimation accuracy.

According to the research on the above methods, this paper proposes a LIB SOH estimation method based on isobaric energy analysis and the modified LSTM NN. First, the isobaric energy curve is derived by analyzing the battery energy variation during the constant current charging phase. Then, the average peak is extracted as the health factor to characterize the aging of LIB SOH. Particle swarm optimization (PSO) is utilized to adjust the learning rate and the number of hidden layers of the LSTM NN in order to build an accurate SOH estimation model. The SOH estimation capability of the proposed method is validated based on different aging data. Experimental results indicate that the method has good estimation capability and stability for battery SOH with four different charging and discharging rates. In addition, the proposed method is compared with the widely used machine learning algorithms to increase the convincing power of the excellent estimation performance for the proposed method. Specifically, several key contributions are presented below.

(1) The isobaric energy analysis method is developed, which can extract efficient health factors.

(2) The optimized LSTM network is constructed through the PSO algorithm filtrates the learning rate and the number of hidden layers of LSTM NN.

(3) The proposed method evidently can be easily generalized to the SOH estimation of other types of batteries without understanding the battery mechanism.

This paper is organized as follows. The isobaric energy analysis and the PSO-LSTM approaches, respectively, are presented in Sections 2 and 3. The background of the experimental setup is provided in Section 4. Lastly, Section 5 summarizes the paper.

2. Isobaric Energy Analysis

Isobaric energy analysis refers to the process of extracting a more effective characterization of battery aging by observing the energy change brought about by charging an equal amount of voltage during constant current charging. To observe the energy change more visually, it is necessary to plot the isobaric energy curve according to

$$E = f(V),$$
$$\frac{\mathrm{d}E}{\mathrm{d}V} = \frac{\Delta E}{\Delta V}, \tag{1}$$

where E and V are the charging energy and voltage, respectively, and $f(\cdot)$ means the function relationship between the energy and voltage.

As an example, take a domestic brand 18650 ternary LIB and draw the isobaric energy curve as shown in Figure 1. It is clear that throughout the constant current charging process, the battery has a significant number of wave peaks. As the wave is being charged and discharged, the wave's position steadily falls. This demonstrates a significant relationship between the battery SOH and the height of wave peaks. As a result, the isobaric energy curve's wave peaks can be used to characterize the battery's aging process. However, as shown in Figure 1, there may be multiple wave peaks in the isobaric energy curve. All of these wave peaks are correlated with the battery SOH. Accordingly, in order to characterize battery aging more accurately, this paper proposes to extract the mean value of the wave peaks as a new health factor to characterize battery aging.

3. SOH Estimation Methodology

3.1. LSTM NN. LSTM NN is designed to overcome the phenomenon of gradient disappearance or gradient explosion in recurrent neural networks for long-time series prediction problems [31]. By combining the nonlinear and data-dependent control units into the recurrent neural network units, LSTM NN keeps the objective function associated with the state signal from vanishing in gradient. Figure 2 depicts the basic structure of the LSTM NN.

The LSTM NN mainly consists of input gate, output gate, and forget gate. While the input gate removes the key information to be retained in the internal state, the forget gate discards the redundant information, and it is the output gate that decides the information to be output. Accordingly, the LSTM NN preserves and updates the key information efficiently over a longer period of time. It is represented below for each gate function and state transfer process in the LSTM module [32].

$$\begin{aligned} f_t &= \sigma\left(w_f \cdot \left[h_{t-1}, x_t\right] + b_f\right), \\ i_t &= \sigma\left(w_i \cdot \left[h_{t-1}, x_t\right] + b_i\right), \\ g_t &= \tan h\left(w_g \cdot \left[h_{t-1}, x_t\right] + b_g\right), \\ o_t &= \sigma\left(w_o \cdot \left[h_{t-1}, x_t\right] + b_o\right), \\ S_t &= f_t \cdot S_{t-1} + i_t \cdot g_t, \\ h_t &= o_t \cdot \delta\left(S_t\right), \end{aligned} \tag{2}$$

where f, i, h, and o are the forget gate, input gate, hidden layer, and output gate, respectively; w represents the input weight; u indicates the recurrent weight; b refers to the bias; σ is the sigmoid function which activates the three gates; and tan$h$ expresses the hyperbolic tangent function.

$$\begin{aligned} \sigma(x) &= \frac{1}{1+e^{-x}}, \\ \tan h(x) &= \frac{e^{x}-e^{-x}}{e^{x}+e^{-x}}. \end{aligned} \tag{3}$$

The learning rate of LSTM NN has a great impact on the model, which determines the learning process of the model and affects whether the objective function converges to the optimal solution. A large learning rate can easily lead to oscillations in the output of the algorithm, while a low learning rate results in overfitting and slow conversion. Therefore, an appropriate learning rate is very important [33]. The hidden layer count directly affects the model accuracy. PSO, a parametric optimization technique that is frequently used, is effective in locating the best solution to typical situations. Consequently, LSTM NN's learning rate and the number of hidden layers are selected using the PSO algorithm.

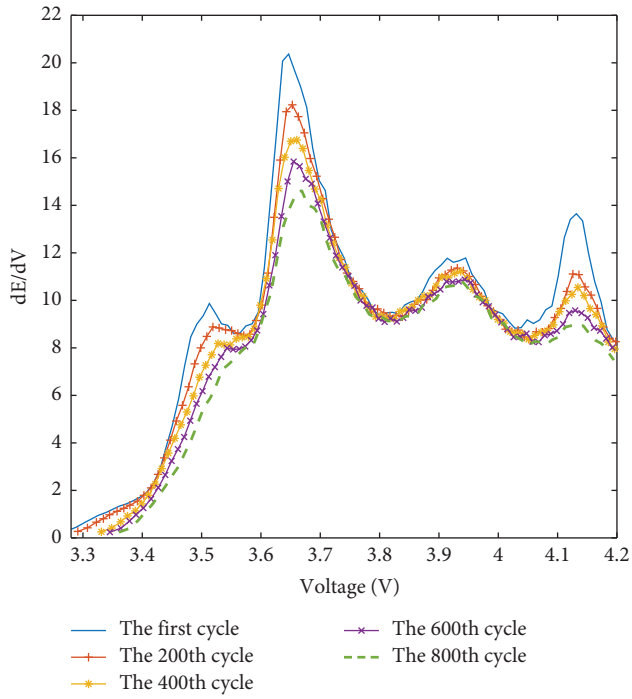

Figure 1: Isobaric energy curve of ternary LIBs.

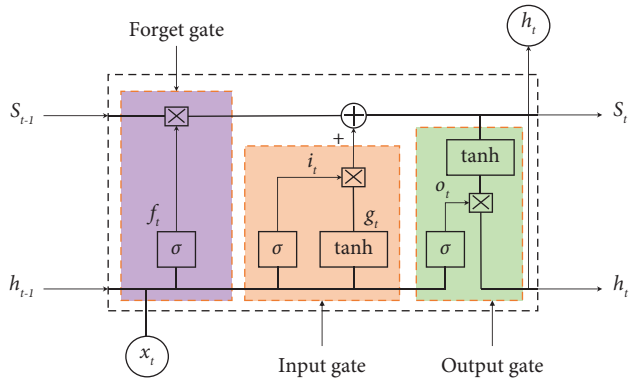

Figure 2: The basic unit of the LSTM.

3.2. PSO Algorithm. The PSO algorithm is a general optimization technique built on the foundation of group search. In many science and engineering fields, it is used to solve nonlinear, nonconvex, or combinatorial optimization issues [34]. It can reach the global optimal solution by the defined fitness function F, accomplished by updating the

generations for the velocity and position of particles. The basic flows of the PSO algorithm in D-dimensional space are as follows [35].

Step 1. Initialize the PSO algorithm including the size of the swarm N and randomly produce the velocity v_i and position x_i of each particle i; v_i and x_i of particle i represent the D-dimensional vector and are defined as

$$\begin{aligned} v_i &= (v_{i1}, v_{i2}, \ldots, v_{iD}), \quad i = 1, \ldots, N, \\ x_i &= (x_{i1}, x_{i2}, \ldots, x_{iD}), \quad i = 1, \ldots, N. \end{aligned} \tag{4}$$

Step 2. Calculate the fitness value $F[i]$ of particle i by the fitness function F.

Step 3. Generate the optimal solution of each particle and global solution by

$$\begin{aligned} p(i) &= \begin{cases} F[i], & F[i] > p(i), \\ & i = 1, \ldots, N, \\ p(i), & \text{otherwise}, \end{cases} \\ g &= \begin{cases} F[i], & F[i] > g, \\ & i = 1, \ldots, N, \\ g, & \text{otherwise}, \end{cases} \end{aligned} \tag{5}$$

where $p_{\text{best}}(i)$ is the optimal position of the particle i and g_{best} represents the optimal position of the particle.

Step 4. Update the velocity and position of particles by

$$v_{iD}^{k+1} = w v_{iD}^{k} + c_1 r_{iD}^{k}\left(p_{iD}^{k} - x_{iD}^{k}\right) + c_2 s_{iD}^{k}\left(g^{k} - x_{iD}^{k}\right), \tag{6}$$

$$x_{iD}^{k+1} = x_{iD}^{k} + v_{iD}^{k+1}, \tag{7}$$

where r and s are random numbers; $k = 1, 2, \ldots, H$ represents the index of the iteration; c_1 and c_2 are constants; and w is referred to as the inertia constant.

Step 5. Repeat steps (2)–(4) until the terminated criterion is met and then exit the program.

3.3. PSO-LSTM Model. The fitness function is the mean absolute error (MAE), which represents the difference between the estimated and true values of the LIB's SOH. The steps of PSO optimization of LSTM NN learning rate and hidden layers number are described as follows:

(1) Initialize PSO algorithm parameters, such as population size, particle index, number of iterations, particle velocity, position, and end conditions. Meanwhile, experience determines the LSTM NN's learning rate and the hidden layer count. The PSO algorithm stops when the error between the true and estimated SOH is less than 1% more than 10 times in a row.

(2) Calculate the fitness value for each particle based on a custom fitness function. The fitness function takes the average absolute error between the estimated and true LIB SOH values.

(3) Generate the local optimal solution and the global optimal solution for each particle, where the local optimal solution is obtained by comparing the actual fitness value of each particle with the historical fitness value. At the same time, the global optimal solution is obtained by comparing the current fitness values of the particles with all the historical fitness values.

(4) Apply (6) and (7), respectively, to update the velocity and location.

(5) Keep going through steps (2) through (4) to attain the algorithm termination condition.

(6) Output the learning rate and hidden layer number of LSTM NN.

4. Experiment Setting and Results

4.1. Experiment Data. The cycle aging experiment was conducted in a laboratory environment using four cylindrical 18650 LIBs with the same specifications. The specific description is as follows:

(1) Constant current charging stage: four LIBs are charged with 0.5 C, 0.3 C, 0.2 C, and 0.1 C current, respectively, until the battery terminal voltage reaches the maximum cutoff voltage of 4.2 V.

(2) Constant voltage charging stage: following constant current charging, the batteries are charged at a constant voltage of 4.2 V until the current drops to 0.1 A.

(3) Discharging stage: the four batteries are discharged at 1 C current until the terminal voltage drops to 3 V.

Each battery's observed aging data are shown in Figure 3, and it is obvious that as a result of repeated charging and discharging cycles and local regeneration events, the battery's discharging capacity gradually declines. This makes it challenging to estimate the LIB SOH.

4.2. Experiment Procedures. SOH estimation experiments were executed with four battery aging curves of different charging multipliers. Figure 4 represents the SOH estimation steps, which are explained as follows:

(1) Plot the isobaric energy curve after analyzing the LIB energy variation in charging stage.

(2) Capture the average peak of the isobaric energy curve. Concurrently, construct the processed dataset and collect the SOH data from the discharging phase.

(3) Divide the processed dataset equally into the training and testing sets. More specifically, suppose the measured historical SOH degradation data and the reported average peak data of the isobaric energy curve for a lithium-ion battery are described as

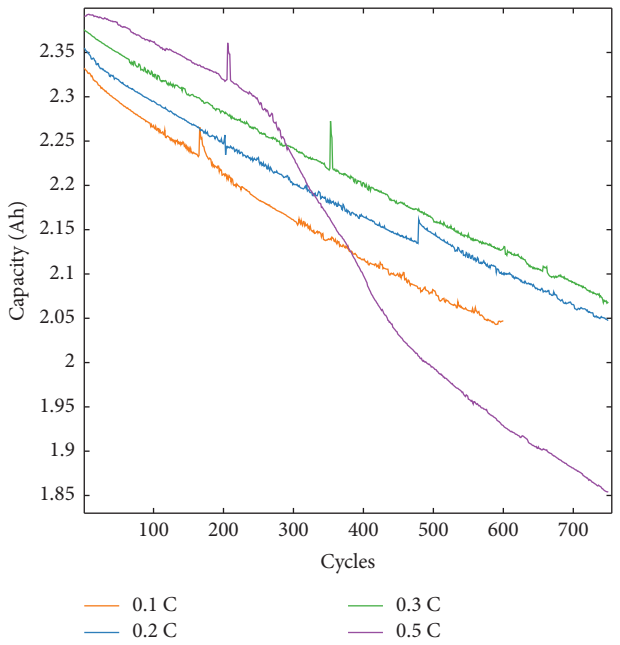

Figure 3: Measured aging data with four different charging ratios.

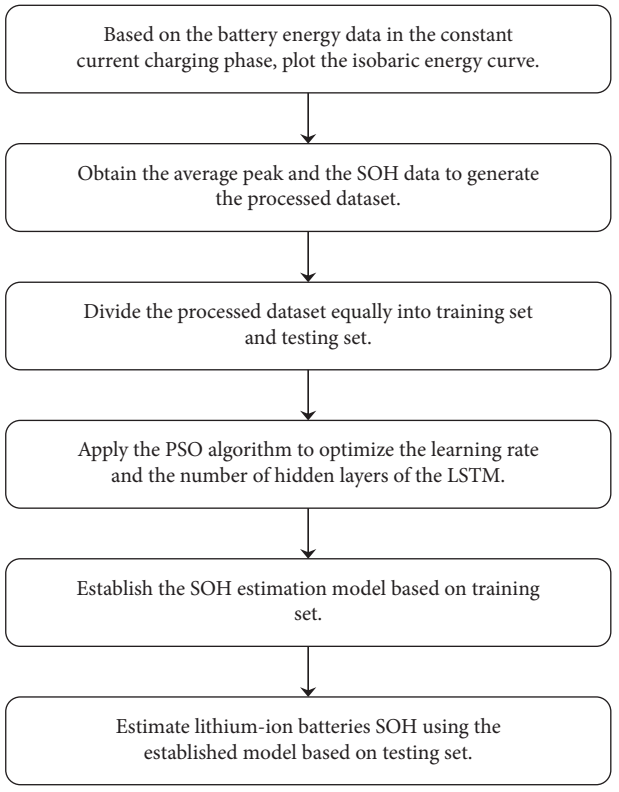

Figure 4: Flowchart of SOH estimation steps.

$$\begin{aligned} \mathrm{SOH} &= \left[\mathrm{SOH}^1, \mathrm{SOH}^2, \ldots, \mathrm{SOH}^m\right]^T, \\ P &= \left[P^1, P^2, \ldots, P^m\right]^T, \end{aligned} \tag{8}$$

where SOH^m indicates the quantified health state in m-th charging and discharging cycle and P^m means the sampled average peak value of the isobaric energy curve in the m-th charging cycle. The training set and testing set are constructed according to

$$\begin{aligned} \text{training set} &= \begin{bmatrix} P^1 & \mathrm{SOH}^1 \\ P^2 & \mathrm{SOH}^2 \\ \vdots & \vdots \\ P^{m/2} & \mathrm{SOH}^{m/2} \end{bmatrix}, \\ \text{testing set} &= \begin{bmatrix} P^{(m/2)+1} & \mathrm{SOH}^{(m/2)+1} \\ P^{(m/2)+2} & \mathrm{SOH}^{(m/2)+2} \\ \vdots & \vdots \\ P^m & \mathrm{SOH}^m \end{bmatrix}, \end{aligned} \tag{9}$$

where $\left[P^1 \quad P^2 \quad \cdots \quad P^{m/2}\right]^T$ refers to the training sample and $\left[\mathrm{SOH}^1 \quad \mathrm{SOH}^2 \quad \cdots \quad \mathrm{SOH}^{m/2}\right]^T$ is the training target when training the SOH estimation model. For testing the model, $\left[P^{(m/2)+1} \quad P^{(m/2)+2} \quad \cdots \quad P^m\right]^T$ represents the testing sample and $\left[\mathrm{SOH}^{(m/2)+1} \quad \mathrm{SOH}^{(m/2)+2} \quad \cdots \quad \mathrm{SOH}^m\right]^T$ is the testing target.

(4) Utilize SOH data corresponding to the charging and discharging cycle as the training target and the average peak as the training sample. Then, use the PSO algorithm to maximize the learning rate and the hidden layer count in the LSTM NN.

(5) Create the SOH estimate model with the optimal LSTM NN.

(6) Based on the testing set, apply the established LIB SOH estimation model to evaluate the LIB SOH.

4.3. Experiment Results and Analysis

4.3.1. Isobaric Energy Analysis Results. Based on the constant current charging stage data, the isobaric energy curve is calculated as shown in Figure 5. It can be observed that two obvious peaks appear in the isobaric energy curve for 0.5 C, but four more obvious peaks appear in the isobaric energy curves for 0.3 C, 0.2 C, and 0.1 C, which are due to the increase in charging multiplier, making the peaks less likely to appear. With the aging test, the peak of the isobaric energy curve for the four different multiples shifts downward, which indicates a strong correlation between the peak value and the LIB SOH. Therefore, this paper adopts the average peak as the health factor to estimate LIB SOH.

4.3.2. Results of PSO-Optimized LSTM Hyperparameters. The process of PSO algorithm optimizing the learning rate and the hidden layer count of LSTM NN for four different charging rates of aging data is shown in Figure 6.

The optimized LSTM NN learning rates and hidden layer count for the different charging multipliers curves are shown in Table 1. Then, the PSO algorithm applies the LSTM NN to

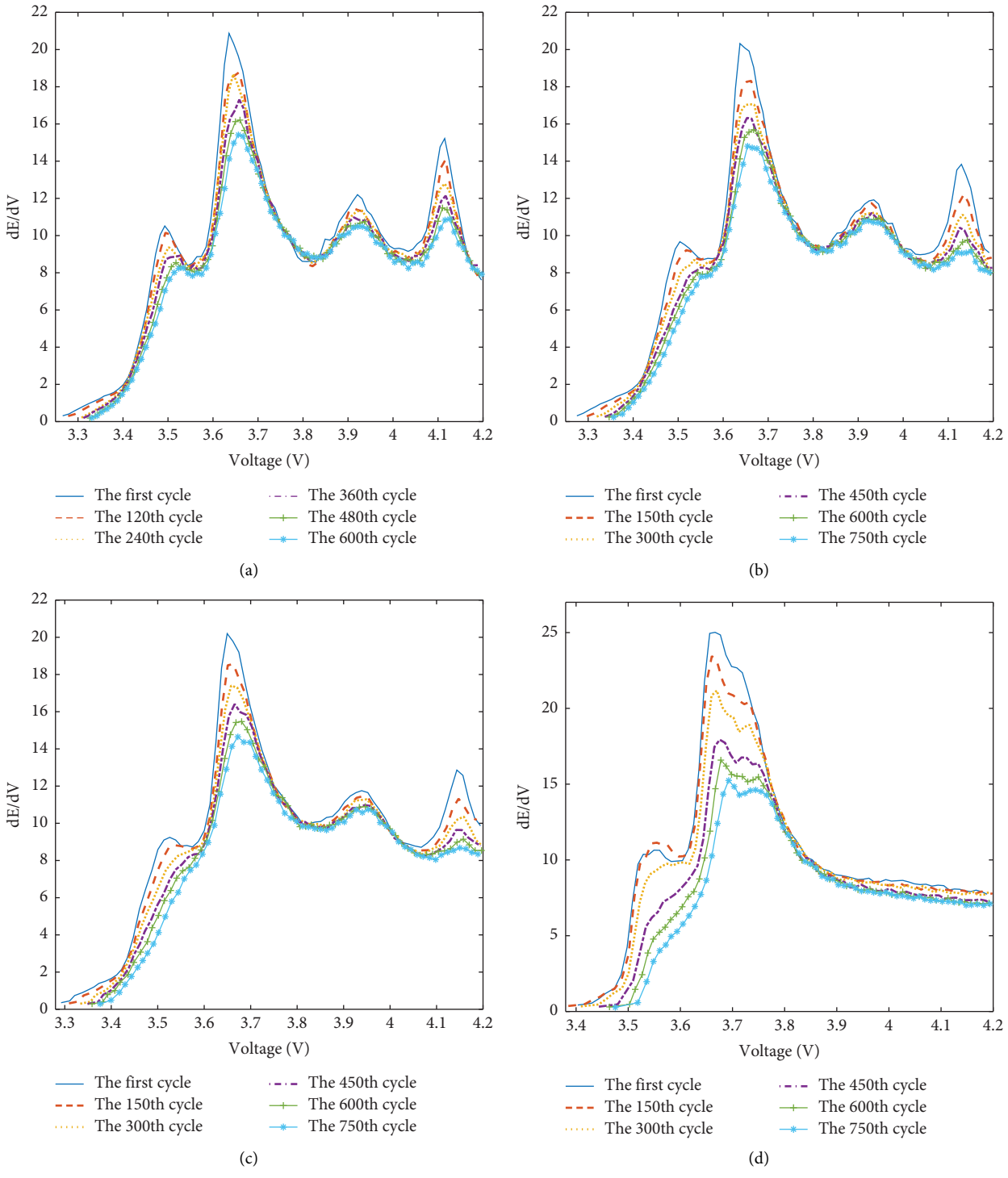

Figure 5: Isobaric energy curves at different charging rates. (a) 0.1 C. (b) 0.2 C. (c) 0.3 C. (d) 0.5 C.

build the LIB SOH estimation model after optimizing the LSTM learning rates and the number of hidden layers.

4.3.3. SOH Estimation Results and Analysis. The established estimation model is applied to evaluate LIB SOH after discharging within the corresponding charging-discharging cycle, using the average peak of the isobaric energy curve obtained during the charge phase within the charging-discharging cycle as input. The experimental results are shown in Figure 7. The proposed method is very close to the real value for different charging multipliers of LIBs and has excellent estimation performance in the results. However, the estimation error gradually increases due to the accumulation of errors. In order to quantify the estimation effect of presented algorithm, evaluation indicators including

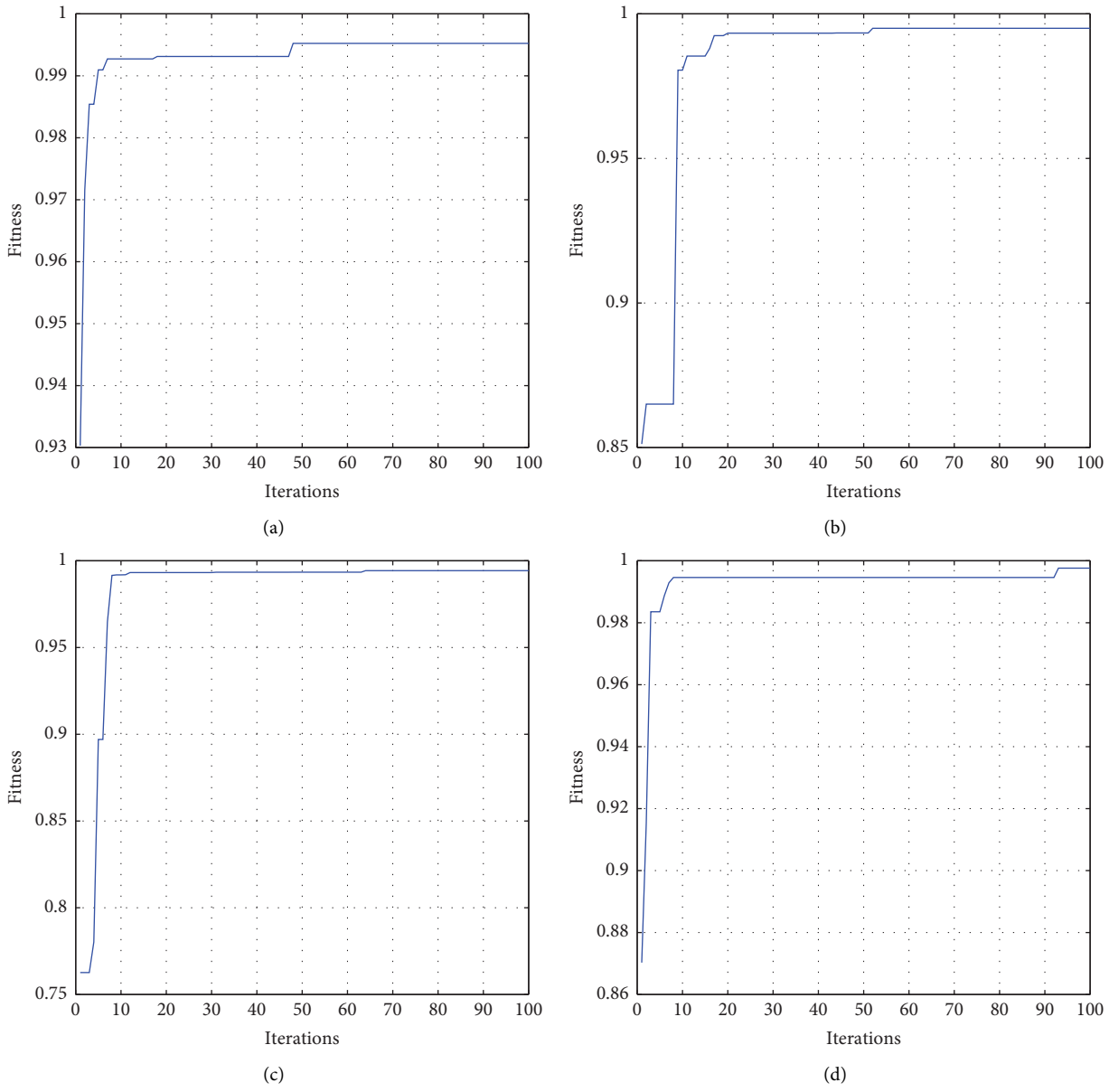

Figure 6: The process of PSO optimizing LSTM hyperparameters. (a) 0.1 C. (b) 0.2 C. (c) 0.3 C. (d) 0.5 C.

Table 1: The selected LSTM NN hyperparameters.

Case	0.1 C	0.2 C	0.3 C	0.5 C
Learning rate	0.001	0.0063	0.0059	0.0025
Number of hidden layers	20	15	10	20

MAE and root mean square error (RMSE) are introduced. The estimation errors are recorded in Table 2. It can be observed that for the four types of aging curves with different charging multipliers, the MAE of the proposed method is less than 1%, which shows excellent estimation performance. In addition, the estimation errors of the charging curves with charging multipliers of 0.2 C and 0.5 C are larger than those of the other two cases due to the stronger nonlinearity of the charging curves with charging multipliers of 0.2 C and 0.5 C.

4.3.4. SOH Estimation Results and Analysis for the Comparison Experiment. A comparison experiment is designed with four kinds of aging curves to further verify the stability and generality of the developed LIB SOH estimation method. It is carried out using commonly used SOH estimation algorithms such as SVM and RVR. Similarly, MAE and RMSE are used as evaluation indicators. The experimental results are presented in Figure 8. Meanwhile, the comparison experiment errors are recorded in Table 3.

By comparing the proposed method with the commonly used SVM and RVR algorithms, it can be concluded that the proposed algorithm outperforms both SVM and RVR for battery aging data with four different charging multipliers. It is because the LSTM NN has excellent time series prediction ability. In this paper, the average peak of the isobaric energy curve is proposed as the health factor, and the learning rate

Table 2: SOH estimation errors of the proposed method.

Case	0.1 C	0.2 C	0.3 C	0.5 C
MAE (%)	0.2819	0.6037	0.4216	0.6076
RMSE (%)	0.3239	0.65	0.4449	0.6720

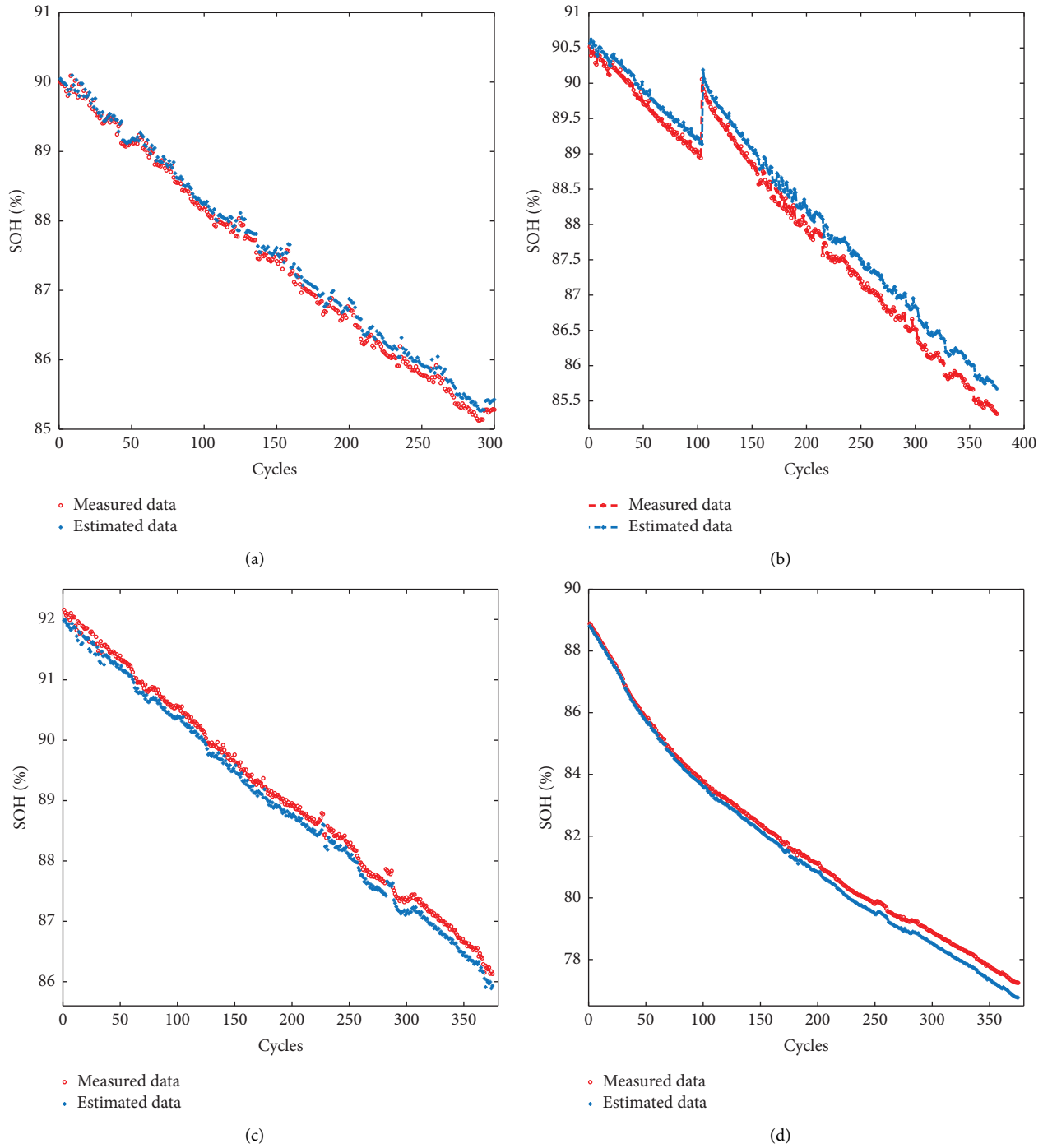

Figure 7: SOH estimation results for the four types of aging data. (a) 0.1 C. (b) 0.2 C. (c) 0.3 C. (d) 0.5 C.

and the number of hidden layers of the traditional LSTM NN are preferred by PSO algorithm. This further enhances the nonlinear regression modeling capability of the LSTM NN. Meanwhile, the error statistics demonstrate that the proposed algorithm has good SOH estimation capability and high robustness and stability. Regarding the 0.5 C charging

Table 3: Estimation errors of the comparative experiment.

Case (C)	Proposed method		SVM		RVR	
	MAE (%)	RMSE (%)	MAE (%)	RMSE (%)	MAE (%)	RMSE (%)
0.1	0.2819	0.3239	1.4159	1.4646	1.5012	1.5789
0.2	0.6037	0.65	1.6043	1.6655	1.7305	1.8176
0.3	0.4216	0.4449	1.3590	1.3545	1.6564	1.7515
0.5	0.6076	0.6720	1.4031	1.4386	1.5101	1.6841

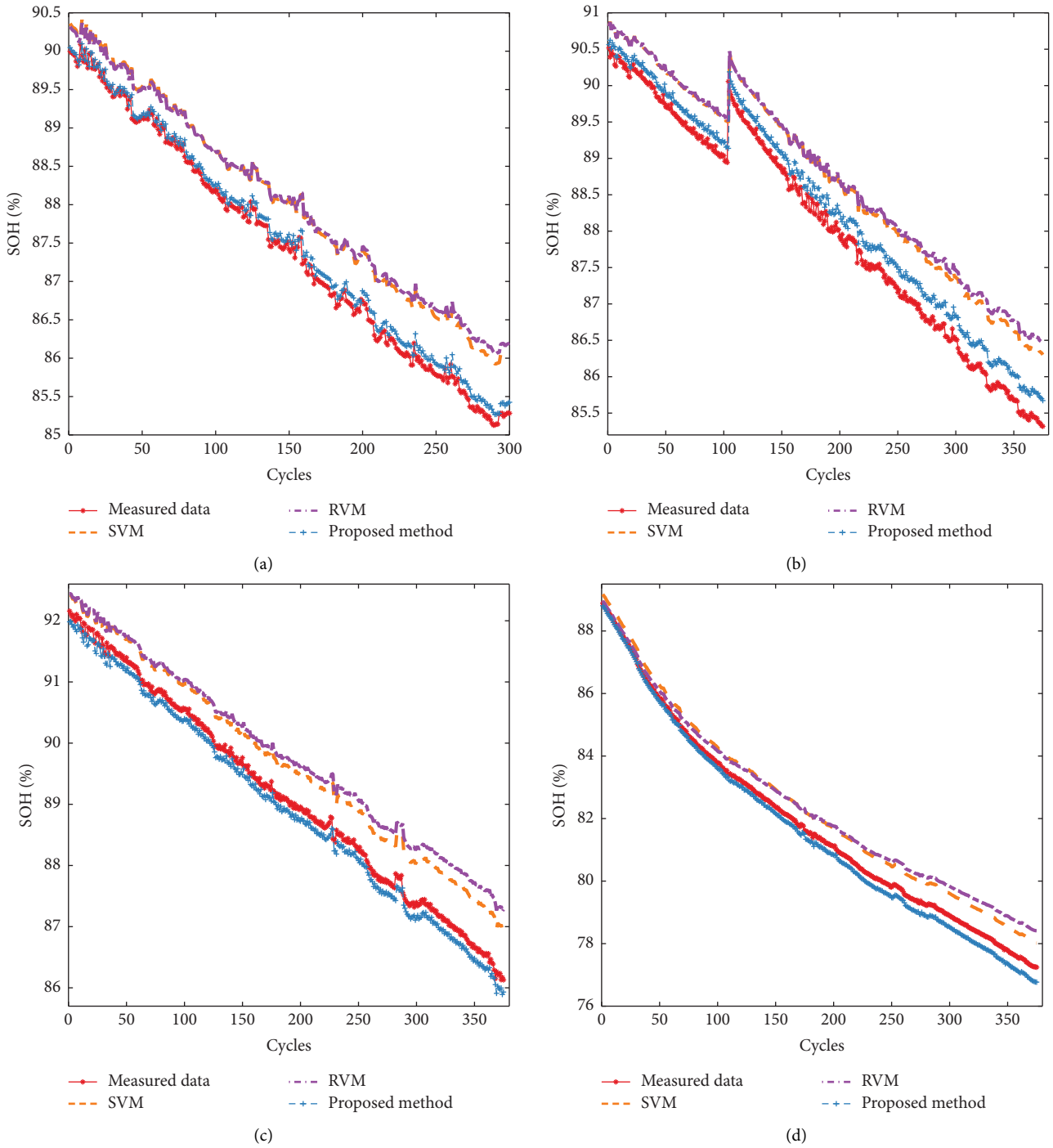

Figure 8: Estimation results of the comparative experiment. (a) 0.1 C. (b) 0.2 C. (c) 0.3 C. (d) 0.5 C.

curve with the strongest nonlinear characteristics, both MAE and RMSE are 0.6076% and 0.6720% of the proposed method, respectively, while the estimation errors of SVM and RVR are around 1.5%, which illustrates that the proposed method's estimation accuracy is much better than that of the commonly used SVM and RVR. As for the 0.2 C charging curve with severe abrupt changes, the proposed method is able to capture the battery SOH variation much faster than the RVR and SVM. This indicates that the method is well adapted to the LIB capacity regeneration phenomenon. For the 0.1 C and 0.3 C charging curves where the aging process is relatively smooth, it has excellent estimation accuracy, with MAE and RMSE no higher than 0.5%. In summary, the LIB SOH estimation algorithm presented in this paper can effectively estimate the SOH of LIBs with good robustness and generalizability.

5. Conclusions

A method for LIB SOH estimation using isobaric energy analysis and PSO-LSTM method has been developed in this paper. Firstly, the evolution pattern of battery energy during the constant-current charging stage has been analyzed and the isovoltaic voltage curves have been plotteds. Then, the variation law of isobaric energy curve with battery degradation has been analyzed, and the average peak has been extracted as the new health factor of battery SOH. Finally, LSTM NN has been optimized in terms of the hidden layer quantities and learning rates using the PSO method, which established the LIB SOH estimation model. The robustness and stability of the proposed method have been verified based on cyclic aging data with four different charging/discharging ratios.

Experimental results have illustrated that the developed method can precisely estimate the LIB SOH with an average estimation error of 1%. It has a superior ability to capture the sudden change of LIB capacity phenomenon. Meanwhile, a comparison experiment has been designed based on the commonly used LIB SOH estimation algorithms, in which the proposed method has been compared with RVR and SVM algorithms. The results indicate that the proposed method has a better estimation performance and good robustness and generalizability.

Data Availability

In this research, we measured our own data to develop the algorithm and used the data to validate our algorithm. The data used to support the findings of this study are available from the corresponding author upon request.

Conflicts of Interest

The authors declare that they have no conflicts of interest.

Acknowledgments

This work was supported by the Anhui Provincial Natural Science Foundation under grant no. 2008085MF197 and Anhui Province Postgraduate Innovation and Entrepreneurship Practice under grant no. 2022cxcysj161.

References

[1] L. Mauler, F. Duffner, W. Zeier, and J. Leker, "Battery cost forecasting: a review of methods and results with an outlook to 2050," *Energy & Environmental Science*, vol. 14, no. 9, pp. 4712–4739, 2021.

[2] S. Hasib, S. Islam, R. Chakrabortty et al., "A comprehensive review of available battery datasets, RUL prediction approaches, and advanced battery management," *IEEE Access*, vol. 9, pp. 86166–86193, 2021.

[3] Y. Yang, E. Okonkwo, G. Huang, S. Xu, W. Sun, and Y. He, "On the sustainability of lithium ion battery industry–A review and perspective," *Energy Storage Materials*, vol. 36, pp. 186–212, 2021.

[4] P. Chombo and Y. Laoonual, "A review of safety strategies of a Li-ion battery," *Journal of Power Sources*, vol. 478, Article ID 228649, 2020.

[5] M. Hossain Lipu, M. Hannan, T. Karim et al., "Intelligent algorithms and control strategies for battery management system in electric vehicles: progress, challenges and future outlook," *Journal of Cleaner Production*, vol. 292, Article ID 126044, 2021.

[6] C. Chen, F. Brosa Planella, K. O'regan, D. Gastol, W. Widanage, and E. Kendrick, "Development of experimental techniques for parameterization of multi-scale lithium-ion battery models," *Journal of the Electrochemical Society*, vol. 167, no. 8, Article ID 80534, 2020.

[7] G. Saldaña, J. San Martín, I. Zamora, F. Asensio, and O. Oñederra, "Analysis of the current electric battery models for electric vehicle simulation," *Energies*, vol. 12, no. 14, p. 2750, 2019.

[8] S. Madani, E. Schaltz, and S. Knudsen Kær, "An electrical equivalent circuit model of a lithium titanate oxide battery," *Batteries*, vol. 5, no. 1, p. 31, 2019.

[9] R. Xiong, L. Li, Z. Li, Q. Yu, and H. Mu, "An electrochemical model based degradation state identification method of Lithium-ion battery for all-climate electric vehicles application," *Applied Energy*, vol. 219, pp. 264–275, 2018.

[10] A. Mevawalla, S. Panchal, M. Tran, M. Fowler, and R. Fraser, "One dimensional fast computational partial differential model for heat transfer in lithium-ion batteries," *Journal of Energy Storage*, vol. 37, Article ID 102471, 2021.

[11] J. Yang, Y. Cai, C. Pan, and C. Mi, "A novel resistor-inductor network-based equivalent circuit model of lithium-ion batteries under constant-voltage charging condition," *Applied Energy*, vol. 254, Article ID 113726, 2019.

[12] Y. Zheng, Y. Cui, X. Han, and M. Ouyang, "A capacity prediction framework for lithium-ion batteries using fusion prediction of empirical model and data-driven method," *Energy*, vol. 237, Article ID 121556, 2021.

[13] K. Severson, P. Attia, N. Jin et al., "Data-driven prediction of battery cycle life before capacity degradation," *Nature Energy*, vol. 4, no. 5, pp. 383–391, 2019.

[14] Y. Zhu, F. Yan, J. Kang, and C. Du, "State of health estimation based on OS-ELM for lithium-ion batteries," *International Journal of Electrochemical Science*, vol. 12, no. 7, pp. 6895–6907, 2017.

[15] T. Sun, R. Wu, Y. Cui, and Y. Zheng, "Sequent extended Kalman filter capacity estimation method for lithium-ion batteries based on discrete battery aging model and support vector machine," *Journal of Energy Storage*, vol. 39, Article ID 102594, 2021.

[16] C. Zhang, Y. He, L. Yuan, and S. Xiang, "Capacity prognostics of lithium-ion batteries using EMD denoising and multiple kernel RVM," *IEEE Access*, vol. 5, pp. 12061–12070, 2017.
[17] L. Mao, J. Xu, J. Chen, J. Zhao, Y. Wu, and F. Yao, "A LSTM-STW and GS-LM fusion method for lithium-ion battery RUL prediction based on EEMD," *Energies*, vol. 13, no. 9, p. 2380, 2020.
[18] L. Yao, S. Xu, Y. Xiao et al., "Fault identification of lithium-ion battery pack for electric vehicle based on ga optimized ELM neural network," *IEEE Access*, vol. 10, pp. 15007–15022, 2022.
[19] J. Nan, B. Deng, W. Cao, and Z. Tan, "Prediction for the remaining useful life of lithium–ion battery based on RVM-GM with dynamic size of moving window," *World Electric Vehicle Journal*, vol. 13, no. 2, p. 25, 2022.
[20] L. Yao, S. Xu, A. Tang et al., "A review of lithium-ion battery state of health estimation and prediction methods," *World Electric Vehicle Journal*, vol. 12, no. 3, p. 113, 2021.
[21] C. Lin, J. Xu, M. Shi et al., "Constant current charging time based fast state-of-health estimation for lithium-ion batteries," *Energy*, vol. 247, Article ID 123556, 2022.
[22] J. Liu and Z. Chen, "Remaining useful life prediction of lithium-ion batteries based on health indicator and Gaussian process regression model," *IEEE Access*, vol. 7, pp. 39474–39484, 2019.
[23] H. H. Goh, Z. Lan, D. Zhang, W. Dai, T. A. Kurniawan, and K. C. Goh, "Estimation of the state of health (SOH) of batteries using discrete curvature feature extraction," *Journal of Energy Storage*, vol. 50, Article ID 104646, 2022.
[24] X. Shu, G. Li, J. Shen, Z. Lei, Z. Chen, and Y. Liu, "A uniform estimation framework for state of health of lithium-ion batteries considering feature extraction and parameters optimization," *Energy*, vol. 204, Article ID 117957, 2020.
[25] S. Pelletier, O. Jabali, G. Laporte, and M. Veneroni, "Battery degradation and behaviour for electric vehicles: review and numerical analyses of several models," *Transportation Research Part B: Methodological*, vol. 103, pp. 158–187, 2017.
[26] X. Han, L. Lu, Y. Zheng et al., "A review on the key issues of the lithium ion battery degradation among the whole life cycle," *eTransportation*, vol. 1, Article ID 100005, 2019.
[27] Y. F. Guo, K. Huang, and X. Y. Hu, "A state-of-health estimation method of lithium-ion batteries based on multi-feature extracted from constant current charging curve," *Journal of Energy Storage*, vol. 36, Article ID 102372, 2021.
[28] D. I. Stroe and E. Schaltz, "Lithium-ion battery state-of-health estimation using the incremental capacity analysis technique," *IEEE Transactions on Industry Applications*, vol. 56, no. 1, pp. 678–685, 2020.
[29] C. Zhang, S. Zhao, Z. Yang, and Y. Chen, "A reliable data-driven state-of-health estimation model for lithium-ion batteries in electric vehicles," *Frontiers in Energy Research*, vol. 10, Article ID 1013800, 2022.
[30] X. Li, C. Yuan, and Z. Wang, "State of health estimation for Li-ion battery via partial incremental capacity analysis based on support vector regression," *Energy*, vol. 203, Article ID 117852, 2020.
[31] Y. Yu, X. Si, C. Hu, and J. Zhang, "A review of recurrent neural networks: LSTM cells and network architectures," *Neural Computation*, vol. 31, no. 7, pp. 1235–1270, 2019.
[32] K. Smagulova and A. James, "A survey on LSTM memristive neural network architectures and applications," *The European Physical Journal- Special Topics*, vol. 228, no. 10, pp. 2313–2324, 2019.
[33] K. Park, Y. Choi, W. J. Choi, H. Ryu, and H. Kim, "LSTM-based battery remaining useful life prediction with multi-channel charging profiles," *IEEE Access*, vol. 8, pp. 20786–20798, 2020.
[34] A. Tharwat and W. Schenck, "A conceptual and practical comparison of PSO-style optimization algorithms," *Expert Systems with Applications*, vol. 167, Article ID 114430, 2021.
[35] Y. Zhu, G. Li, R. Wang, S. Tang, H. Su, and K. Cao, "Intelligent fault diagnosis of hydraulic piston pump combining improved LeNet-5 and PSO hyperparameter optimization," *Applied Acoustics*, vol. 183, Article ID 108336, 2021.